OPTIMIZING STEP-SIZE OF PERTURB & OBSERVE AND INCREMENTAL CONDUCTANCE MPPT TECHNIQUES USING PSO FOR GRID-TIED PV SYSTEM

Sai Shekar Tammineni, Rudru Mary Kamala, Perla Naga Harshini,
Voosavarapu Vamsi
R.V.R. & J.C.College of Engineering, Chandramoulipuram, Chowdavaram, GUNTUR-522 019 Andhra Pradesh :: India

Under the Guidance of
N.Dharani Kumar, Assistant Professor, Department of EEE
R.V.R. & J.C.College of Engineering, Chandramoulipuram, Chowdavaram, GUNTUR-522 019 Andhra Pradesh :: India

ABSTRACT:

A maximum power point tracking (MPPT) technique plays an important role to ensure maximum photovoltaic (PV) output power is extracted under stochastic weather conditions. The research to date tends to focus on developing a standalone optimization MPPT algorithm rather than looking into a hybrid MPPT algorithm. This paper introduces particle swarm optimization (PSO) to optimize the maximum PV output power and to determine the best design variable for penalizing the step size of the conventional methods namely the perturb and observe (PO) and the incremental conductance (IC). With the help of the hybrid MPPT algorithm (PSO+IC and PSO+PO), the step size is no longer fixed, and it is changing according to the solar irradiance. To evaluate the proposed hybrid algorithm, a single-stage grid connected PV system is designed for several different scenarios with various weather conditions. The performance of the hybrid MPPT algorithm and the conventional methods is compared. The results demonstrate that the hybrid MPPT algorithm is remarkably better than the conventional methods, especially for PSO+IC, where it only takes 43.4 ms of tracking time and reaches the efficiency of 99.07% under standard test conditions.

INDEX TERMS - Hybrid MPPT, particle swarm optimization, incremental conductance, perturb and observe, optimal step-size, single-stage grid connected PV system.

I. INTRODUCTION:

Due to the rising economic development and energy consumption, photovoltaic (PV) systems have been widely used in industry. One significant advantage of employing PV systems is that the sources are clean and less harmful to the environment compared to conventional power generation [1]. The ability of PV systems to reduce greenhouse gas emissions while producing power has made this system more reliable and robust. There

are two widely used grid-tied inverters namely single-stage and double-stage inverters [2]. Singlestage grid connected PV systems comprise of dc/ac inverter with a transformer. Meanwhile, double-stage grid connected PV systems comprise of dc/ac inverter with a dc/dc boost converter. The power generation of the PV system highly depends on the weather conditions (i.e. solar irradiance and temperature), such that the output power will fluctuate due to the stochastic weather condition. Furthermore, the current against voltage and power against voltage curve shows a nonlinear relationship of the PV module. Thus, to harvest maximum power from the PV system, the maximum power point tracking (MPPT) algorithm is required and plays an important role in the PV system as discussed in [3]. Many researchers had proposed different types of algorithms and artificial intelligence techniques to determine the MPPT of the PV system. The most well-known algorithms used are the perturb and observe, and the incremental conductance. These methods are easy to implement and depend on the step change of the voltage or duty cycle [4]. Perturb and observe algorithm is based on the derivative of power in function of voltage is equal to zero at the maximum power point, meanwhile, the incremental conductance algorithm is based on comparing the values between PV array instantaneous current against voltage with the derivative of current in the function of voltage [5]. On the other hand, the artificial intelligence approach could be developed based on maximising the output power of the PV array. In recent years, a modified MPPT algorithm was developed by many researchers with different applications which will be discussed as follows. In [6] and [7], an improved MPPT algorithm was developed based on the conventional incremental conductance and employed in a boost converter circuit. In [8] and [9], a modified incremental conductance was employed in a single-stage grid connected PV system. In [10], an improved perturb and observe algorithm was proposed and employed in the buck-boost converter circuit. In [11], a two-stage MPPT algorithm was proposed based on adaptive scaling factor beta, and perturb and observe algorithm was proposed and employed in the boost converter circuit. In [12], an improved variable step size of perturb and observe MPPT algorithm was developed and employed in the boost converter circuit. In [13], a modified perturb and observe MPPT was proposed and employed in a doublestage grid connected PV system. In [14], a high-performance variable step size perturb and observe MPPT algorithm was proposed and employed in a buck converter circuit. In [15], an improved MPPT control strategy was developed based on incremental conductance and was employed in the boost converter circuit. In [16], fast tracking incremental conductance algorithm was proposed and employed in the boost converter circuit. However, employing such an algorithm as discussed beforehand, highly depends on the step size

voltage or duty cycle. Moreover, these techniques may not provide accurate tracking of the maximum power point (MPP) and it may result in an oscillation of voltage near the maximum power point. Therefore, to overcome these problems, optimization techniques had been widely developed by many researchers. One major advantage of employing optimization techniques is the ability of the algorithm to determine the global optimum solution by generating random variables in the search space [17]. The capability of optimization techniques in many applications has made other researchers consider these methods to develop a better MPPT algorithm. In the past few years, many researchers have proposed an MPPT algorithm based on optimization techniques which will be discussed as follows. In [18], particle swarm optimization (PSO) has been employed to determine the MPPT by proposing two additional conditions namely the convergence detection and the change in solar insolation detection. In [19], an improved PSO-based MPPT was developed to reduce the steady state oscillation. In [20], the water cycle algorithm MPPT with the characteristics of power and current was proposed. In [21], a PSO-based global MPPT technique for distributed PV power generation with constraints for boost converters was proposed. In [22], a novel MPPT was proposed based on the Lagrange interpolation formula and PSO method. In [23], improved PSO, and perturb and observe MPPT algorithm were developed to reduce the oscillation during the MPPT phase. In [24], overall distribution and PSO MPPT algorithm were proposed to improve the tracking speed for maximum power point. In [25], a hybrid adaptive neuro-fuzzy inference system (ANFIS) and PSO-based MPPT method were proposed and employed in a zeta converter circuit to obtain rapid and zero oscillation tracking. In [26], an improved grey wolf optimizer MPPT algorithm was proposed and employed in boost full-bridge isolated converter (BFBIC) topology. In [27], an improved MPPT algorithm based on the earthquake optimization algorithm was proposed and employed in boost converter circuit to improve the dynamic behaviour of the PV systems. In [28], incremental conductance based on the PSO algorithm for MPPT was proposed and employed in the boost converter circuit. As discussed beforehand, most researchers tend to focus on developing a standalone optimization MPPT algorithm. The combination of optimization techniques and the conventional MPPT algorithms in standalone PV systems have shown improvement in the overall performance of the system [23], [28]. However, less effort is put into the work in integrating optimization techniques and the conventional methods for single-stage grid connected PV systems. It is expected to provide faster and more accurate tracking MPP which can improve the overall efficiency of the system. In addition, it can also make the system more robust and can adapt to different operating conditions. In

this paper, the method of improving the conventional methods namely the perturb and observe, and the incremental conductance by employing the optimization technique is presented. The method employed is to optimize the maximum PV output power and to determine the best design variable for penalizing the step size of the conventional methods. The results show that the combined methods lead to better efficiency and performance compared to the conventional methods. The remainder of the paper is structured as follows. Section II describes the overview of the conventional MPPT algorithm. Section III describes the overview of the particle swarm optimization. Section IV describes the proposed MPPT algorithm based on particle swarm optimization. Section V provides the implementation and design of the single-stage grid connected PV system. Section VI discusses the results. Finally, Section VII concludes the paper.

II. OVERVIEW OF THE CONVENTIONAL MPPT ALGORITHM

As discussed earlier, the most widely-known MPPT algorithms are the traditional perturb and observe, and incremental conductance. These algorithms are widely used due to their simplicity and effectiveness to track the MPP. Moreover, these algorithms are used as a baseline and they are considered standard references to make any comparisons with new algorithms [14]. In this section, the overviews of both algorithms are discussed.

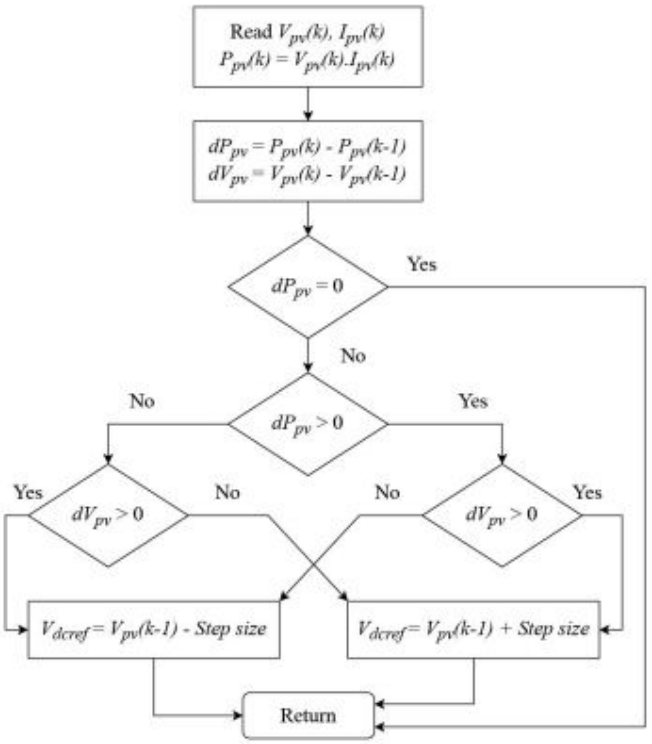

FIGURE 1. Flowchart of the conventional perturb and observe algorithm [14], [30], [33

A. PERTURB AND OBSERVE

Figure 1 shows the flowchart of the conventional perturb and observe algorithm. The voltage and current are measured from the PV module output to calculate the value of the output power. The difference in power and voltage is then calculated between the new values and the previous values. At the maximum operating point the change in power, dPpv, is equal to zero. However, if dPpv is not equal to zero, the algorithm will try to find the best solution by increasing or decreasing the voltage with a fixed step size. If the operating point of the PV is on the left-

hand side, the algorithm will track the MPP by driving the system to the right-hand side near the MPP and vice-versa.

B. INCREMENTAL CONDUCTANCE

Figure 2 shows the flowchart of the incremental conductance algorithm. The voltage and current are measured from the PV module output. The value of change in voltage and current are calculated to determine the derivative of current in voltage. Moreover, the principle of the conventional incremental conductance algorithm is based on comparing the value between the derivative of current in the function of voltage and the PV array instantaneous current against voltage. This algorithm simply tracks the MPP by increasing or decreasing the reference voltage based on the operating point of the system. At MPP, the following conditions

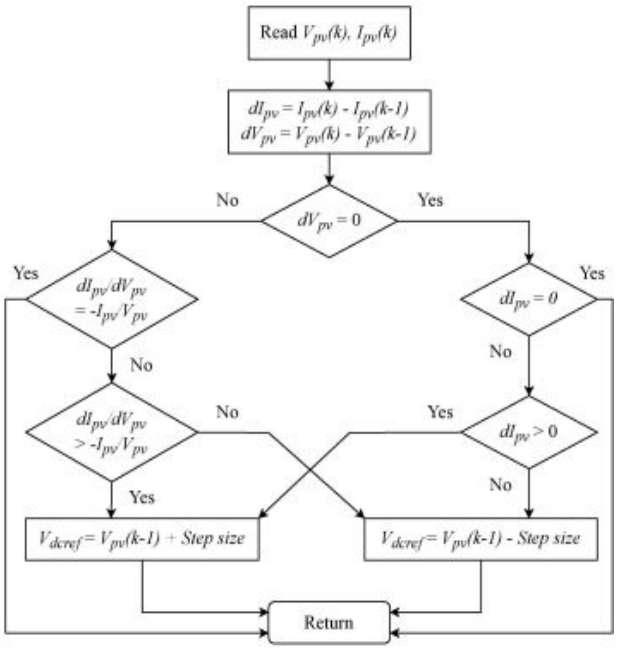

FIGURE 2. Flowchart of the conventional incremental conductance algorithm [31], [32], [33].

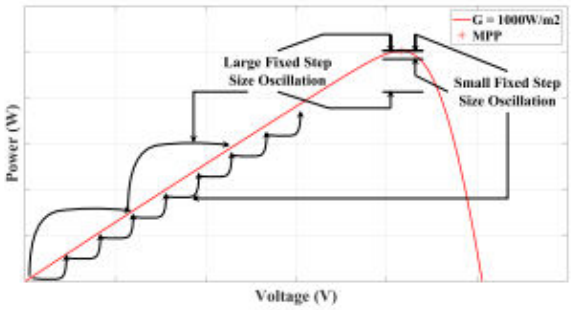

FIGURE 3. Comparison between small and large fixed step sizes oscillation at the MPP.

must be met [31], [32], [33]:

$$\frac{dP}{dV} = 0 \tag{1}$$

$$\frac{dP}{dV} = \frac{d(V \cdot I)}{dV} = I\frac{dV}{dV} + V\frac{dI}{dV} \tag{2}$$

$$\frac{dI}{dV} = -\frac{I}{V} \tag{3}$$

where dI/dV is the derivative of current in the function of voltage, and I/V is the PV instantaneous current against voltage. Furthermore, if dI/dV > 0, the reference voltage is increase based on fixed step voltage. Meanwhile, if dI/dV

< 0 the reference voltage is decrease based on the fixed step voltage. Both algorithms rely heavily on the step size that the user provides. Figure 3 shows the oscillation comparison between small and large fixed step sizes on the power against voltage curve. Small steady state oscillations are accomplished with small step sizes, but at the expense of a poor MPPT time response and a decline in output power efficiency. Meanwhile, using large step sizes enhances the MPPT time response. However, the steady state oscillations near the maximum power point are amplified. Hence, in this paper, optimization is employed to maximize the output of PV power by penalizing and varying the step size which will be discussed further in this paper.

III. OVERVIEW OF PARTICLE SWARM OPTIMIZATION

Particle swarm optimization algorithm can be simply described as fish schooling or a bird flocking searching for food in space, where it uses the velocity vector, the experience of each particle, and the experience of the neighbouring particle to generate a random position vector in the space [29]. The position of each particle in the space can calculated and updated based on the velocity equation given as [29]:

$$E_g = E_{g,ref}(1 - 0.0002677[T_c - T_{ref}]) \quad (13)$$

$$I_o = I_{o,ref}\left[\frac{T_c}{T_{ref}}\right]^3 \exp\left(\frac{1}{k}\left[\frac{E_g}{T_{ref}} - \frac{E_g}{T_c}\right]\right) \quad (14)$$

where Ns is the number of cells in the module, n is the ideality factor, K is the Boltzmann constant, q is the charge of an electron, G is the irradiance, Gref is the irradiance at standard reference condition (SRC), Tc is the temperature, and Tref is the temperature at SRC. In addition, the diode reverse saturation current, Io, can be mathematically expressed as [34]:

$$R_{sh} = R_{sh,ref} \cdot \frac{G_{ref}}{G} \quad (15)$$

where Rsh,ref is the reference parallel resistance at SRC. Moreover, four constraints are taken into consideration. The first constraint is based on current against voltage curve characteristics, where it can be mathematically expressed as:

$$\frac{dI}{dV} = -\frac{1}{R_{sh}} - \frac{qI_o \exp\left(\frac{q(V_{pv} + I_{pv}R_s)}{nKTN_s}\right)}{nKTN_s} \quad (16)$$

where at the MPP, the first derivative of current in the function of voltage which is written in (16), must be equal to the instantaneous PV current divided by the instantaneous PV voltage. The second constraint is based on power against voltage curve characteristics, where it can be mathematically expressed as:

$$\frac{dP}{dV} = I_L - V_{pv}\left(\frac{1}{R_{sh}} + \frac{qI_o \exp\left(\frac{q(V_{pv} + I_{pv}R_s)}{nKTN_s}\right)}{nKTN_s}\right) - \frac{V_{pv} + I_{pv}R_s}{R_{sh}} - I_o\left(\exp\left(\frac{q(V_{pv} + I_{pv}R_s)}{nKTN_s}\right) - 1\right) \quad (17)$$

where at the MPP, the first derivative of power in the function of voltage is equal to zero. Meanwhile, the third and fourth

constraints are to limit the search space of PSO, which can be mathematically expressed as:

$$0 < V_{pv} < V_{pv,max} \quad (18)$$

$$0 < I_{pv} < I_{pv,max} \quad (19)$$

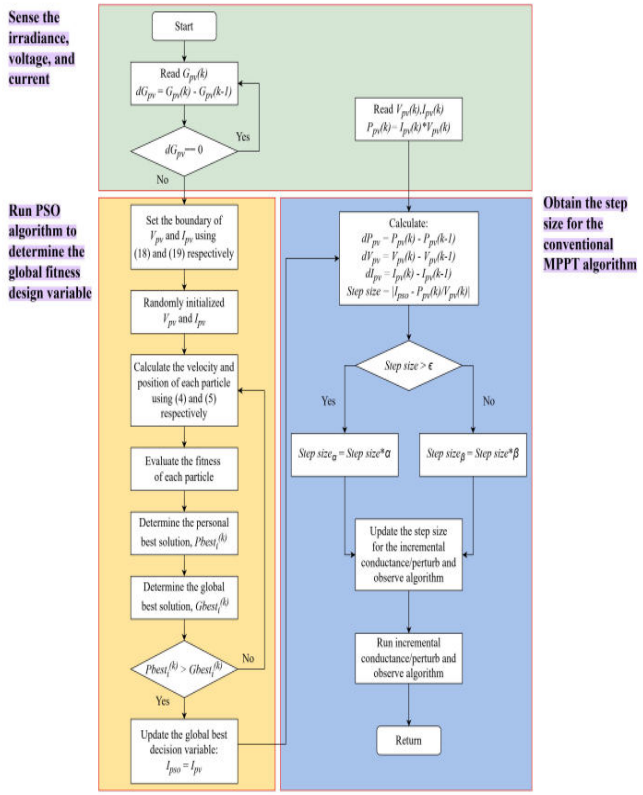

FIGURE 4. Flowchart of the proposed MPPT based on PSO.

where Vpv,max and Ipv,max are the open circuit voltage and the short circuit current of the PV module respectively. At every iteration, PSO will update the best and the global best fitness value ever found in the search space. If the algorithm fails to determine the optimal solution, the decision variables are randomly re-initialized to search for the global best fitness value. The best design variable, Ipso, is then updated for the conventional MPPT algorithm to calculate the step size, which can be expressed as:

$$Step\ size = \left| I_{pso} - \frac{P_{pv}(k)}{V_{pv}(k)} \right| \quad (20)$$

Furthermore, a tolerance, ϵ, is introduced to penalized the step size such that if the step size is greater than ϵ, the new step size can be mathematically expressed as:

$$Step\ size_{\alpha} = Step\ size \times \alpha \quad (21)$$

where α is a large constant such that to enhance the performance of the MPPT by providing faster tracking time of the MPP during the change in weather conditions. Meanwhile, if the step size is less than ϵ, the new step size can be mathematically expressed as:

$$Step\ size_{\beta} = Step\ size \times \beta \quad (22)$$

where β is a small constant such that to enhance the performance of the MPPT by reducing the oscillation near the MPP during the steady-state condition. The calculated step size is then updated for the conventional MPPT algorithm.

V. IMPLEMENTATION AND DESIGN OF SINGLE-STAGE GRID CONNECTED PV SYSTEM

Figure 5 shows the typical single-stage grid connected PV system control scheme. The system consists of a PV panel, dc-link voltage, dc/ac inverter, and LCL filter. The dc-link

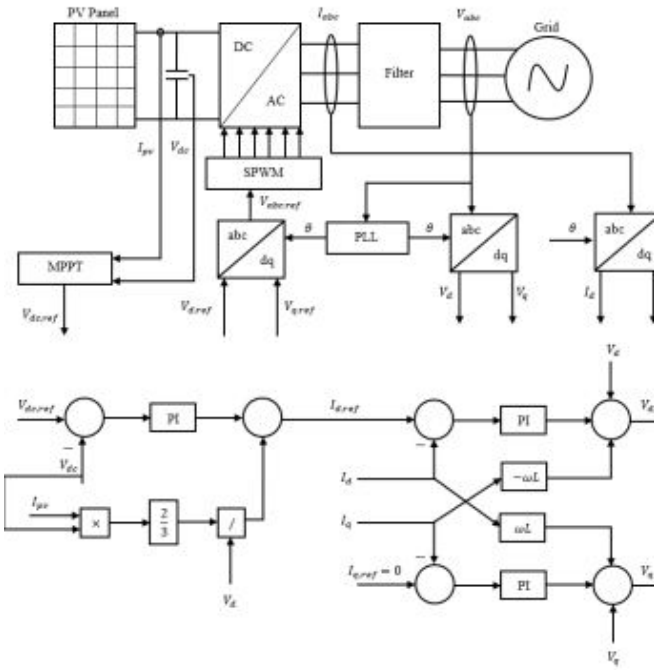

IGURE 5. Single-stage grid connected PV system control scheme [8], 57], [38], [43].

voltage is regulated by using the outer loop voltage control (i.e., feed forward voltage regulator) to achieve low total harmonic distortion in the grid [39]. The outer loop utilises one PI controller to match the dc-link voltage with the reference voltage, Vdc,ref . Meanwhile, the inner loop current control utilises two PI controllers to regulate the direct current, Id , and the quadrature current, Iq. The general relationship between the grid-tied inverter voltages and line currents can be expressed as [39]:

$$\begin{bmatrix} e_a \\ e_b \\ e_c \end{bmatrix} = R_f \begin{bmatrix} I_a \\ I_b \\ I_c \end{bmatrix} + L_f \frac{d}{dt} \begin{bmatrix} I_a \\ I_b \\ I_c \end{bmatrix} + \begin{bmatrix} V_a \\ V_b \\ V_c \end{bmatrix} \quad (23)$$

where ea, eb and ec are the inverter output voltages, Ia, Ib and Ic are the three-phase line currents, Va, Vb and Vc are the three-phase grid voltages, and Rf and Lf are the filter resistance and inductance respectively. The synchronisation of the PV system to the grid is employed by converting three-phase electrical quantities to d-q axis quantities using Park's transformation, in which, a synchronous reference frame based phase-locked loop is employed [44]. The rotating reference frame synchronised with the grid voltage can be mathematically expressed as [39]:

$$V_d = e_d - R_f I_d + \omega L_f I_q - L\frac{dI_d}{dt} \quad (24)$$

$$V_q = e_q - R_f I_q - \omega L_f I_d - L\frac{dI_q}{dt} \quad (25)$$

where Vd and Vq are the grid d-axis and q-axis voltage components respectively, ed and eq are the d-axis and q-axis inverter voltage components respectively, Id and Iq are the daxis and q-axis grid currents respectively, and ω is the grid angular frequency.

TABLE 1. Grid-tied PV array simulation parameters [41], [42].

Parameter	Value
Filter Inductance, $L_{filter,1}$,$L_{filter,2}$	500 μH
Filter Capacitance, C_{filter}	100 μF
DC-link Capacitance, $C_{dc-link}$	1000 μF
Grid Voltage, V_{LL}	415 V
Grid Frequency, f	50 Hz
Inverter Switching Frequency, f_{sw}	10 kHz

TABLE 2. PV module specifications at 1000 W/m^2 and 25 °C [40].

VBHN225SA06B Module Parameter	Value
Maximum Power, P_{mpp}	225.472 W
Cells per module, N_{cell}	72
Open-circuit Voltage, V_{oc}	50.6 V
Short-circuit Current, I_{sc}	5.83 A
Voltage at MPP, V_{mp}	41.6 V
Current at MPP, I_{mp}	5.42 A
Temperature coefficient of V_{oc}	-0.24%/ °C
Temperature coefficient of I_{sc}	0.0020069%/ °C
Light-generated current, I_L	5.8457 A
Diode saturation current, I_D	1.15×10^{-12} A
Diode ideality factor, n	0.93611
Shunt resistance, R_{sh}	242.2585 Ω
Series resistance, R_s	0.65124 Ω
Parallel strings, $N_{parallel}$	1
Series-connected strings, N_{series}	1

TABLE 3. PV array specifications at 1000 W/m^2 and 25 °C [40].

PV Array Parameter	Value
Maximum Power, P_{mpp}	1.003 MW
Open-circuit Voltage, V_{oc}	2530 V
Short-circuit Current, I_{sc}	518.87 A
Voltage at MPP, V_{mp}	2080 V
Current at MPP, I_{mp}	482.38 A

In addition, in the synchronous rotating frame, the real power, Pgrid , and the reactive power, Qgrid , can be expressed as [39]:

$$P_{grid} = \frac{3}{2}(V_d I_d + V_q I_q) \quad (26)$$

$$Q_{grid} = \frac{3}{2}(V_q I_d - V_d I_q) \quad (27)$$

The specification and relevant parameters of the grid-tied PV inverter are shown in Table 1. A Sanyo Electric Co Ltd of Panasonic Group VBHN-225S-A06B PV module is used and its output characteristics at standard test conditions are listed in Table 2. The PV array employed in this paper consists of 89 parallel strings and 50 seriesconnected strings of the VBHN-225S-A06B module. Table 3 shows the specification of the PV array at standard test conditions.

VI. SIMULATION RESULTS AND ANALYSIS

Single stage grid connected PV system is simulated using the MATLAB/Simulink software with different MPPT

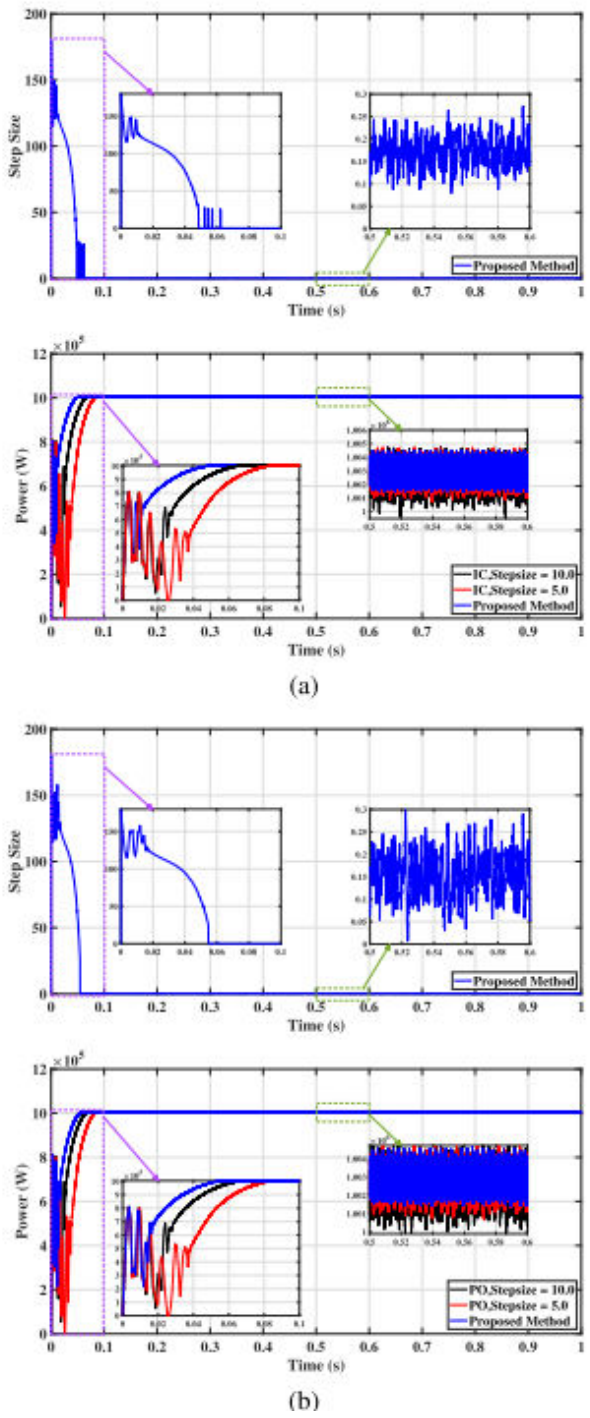

FIGURE 6. System response under standard test conditions; (a) Proposed method step size and PV output power comparison for incremental conductance, and (b) Proposed method step size and PV output power comparison for Perturb and Observe

TABLE 4. Main parameters of the PSO algorithm.

Parameter	Value
Inertia Weight, α	1.0
Cognitive Coefficient, c_1	1.5
Social Coefficient, c_2	1.5

TABLE 5. Standard test conditions performance comparison between the proposed methods and the conventional methods.

MPPT Algorithm	Step Size	Settling Time (ms)	P_{Actual} (MW)	η (%)
IC	5	77.6	0.971	96.85
	10	60.5	0.983	97.98
P&O	5	77.6	0.971	96.85
	10	60.4	0.983	97.98
Proposed IC	0.01 to 180	43.4	0.994	99.07
Proposed P&O	0.01 to 180	49.5	0.990	98.73

A. CASE 1: STANDARD TEST CONDITIONS

The output power with different MPPT algorithms and the step size of the proposed method are shown in Figure 6. It can be seen clearly that for a large fixed step size, the tracking of the MPP is much faster. However, there is a large oscillation of output power at a steady state. Meanwhile, for a small fixed step size, the tracking process is much slower. But, this will reduce the oscillation of output power at a steady state. Moreover, in comparison with the proposed methods, the step size generated varies from a larger step size (180) to a smaller step size (0.01). This improves the performance by providing faster tracking time and increases the efficiency of the output power as shown in Table 5. It must be noted that as the fixed step size of the conventional MPPT increases, the output power efficiency will decrease due to the increase in ripple output power, this affects the system performance in the long run. In addition, the efficiency of the output power, η, for each MPPT algorithm can be expressed as:

where t is the time, PActual is the actual output power generated from the PV system, and PTheoretical is the theoretical output power generated from the PV system. In Table 5, it must be noted that the PTheoretical is equal to 1.003 MW.

B. CASE 2: CHANGING IRRADIANCE CONDITIONS

The changing irradiance is applied to the single stage grid connected PV system with constant temperature (25 oC) as shown in Figure 7(a). The step size of the proposed method and the output power with different MPPT algorithms are shown in Figure 7(b) and 7(c) respectively. The output power of the system demonstrates that the step size provided by the proposed method is more precise in all situations. VOLUME 11, 2023

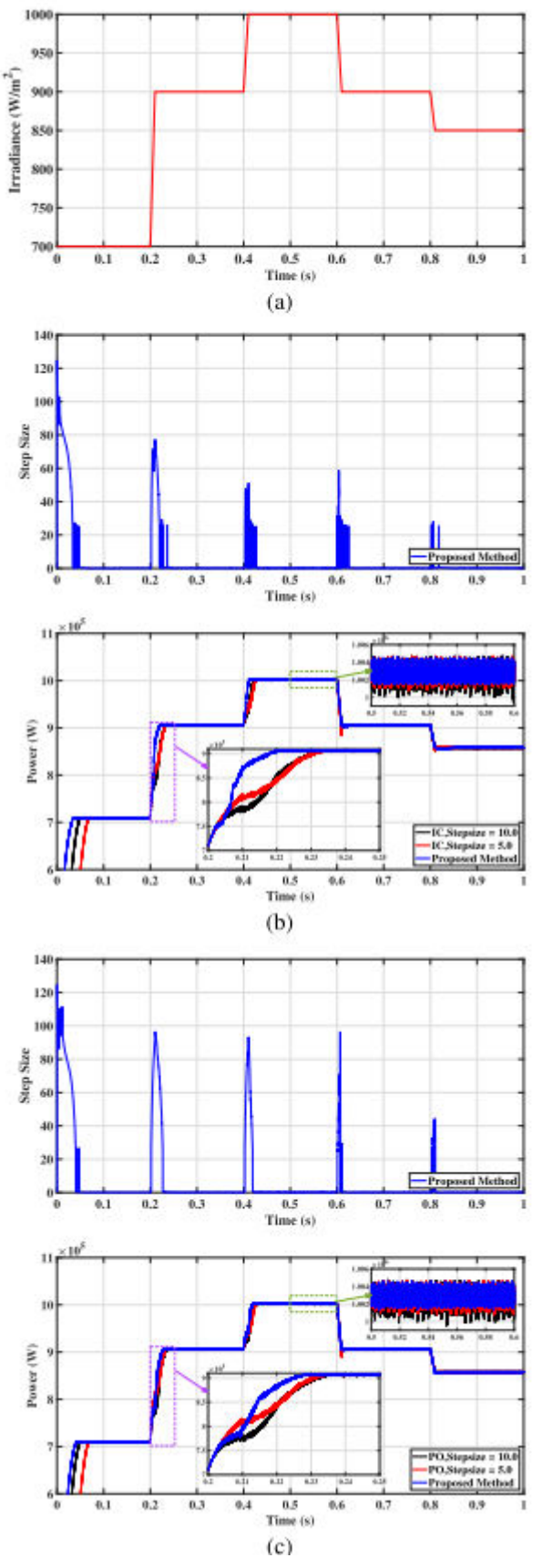

FIGURE 7. System response under changing irradiance conditions; (a) Changing irradiance profile, (b)

Proposed method step size and PV output power comparison for incremental conductance, and (c) Proposed method step size and PV output power comparison for Perturb and Observe.

C. CASE 3: CHANGING TEMPERATURE CONDITIONS

The changing temperature is applied to the same system with constant irradiance (1000 W/m2) as shown in Figure 8(a)

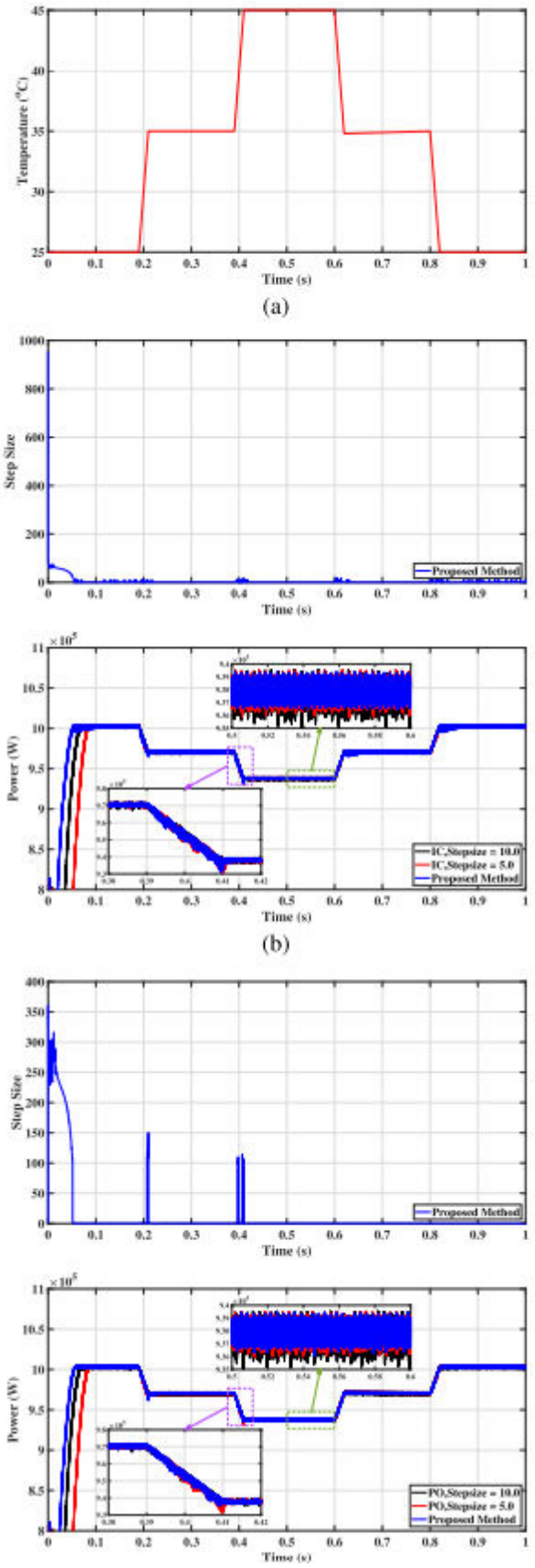

FIGURE 8. System response under changing temperature conditions; (a) Changing temperature profile, (b)

Proposed method step size and PV output power comparison for incremental conductance, and (c) Proposed method step size and PV output power comparison for Perturb and Observe.

The step size of the proposed method and the output power with different MPPT algorithms are shown in Figure 8(b)

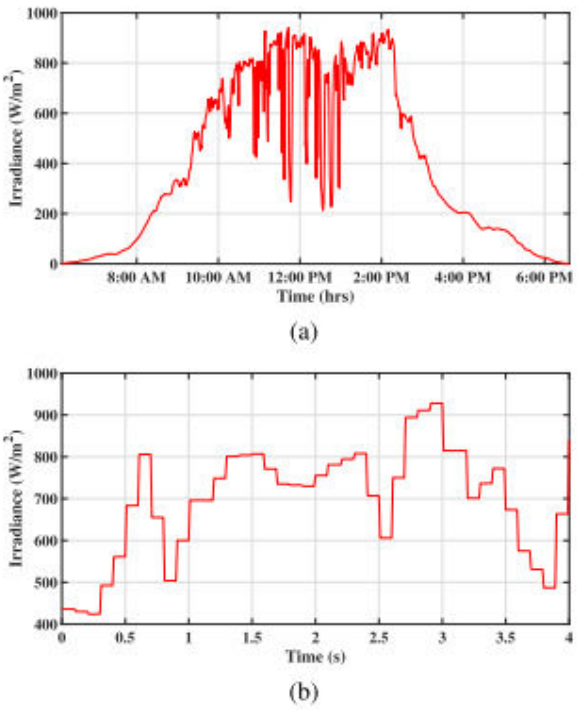

FIGURE 9. (a) Real time irradiance (b) Samples of irradiance.

and 8(c) respectively. The output power of the system demonstrates that the step size provided by the proposed method does not show any significant improvement to the system in terms of tracking time. Yet, the proposed algorithm is capable to reduce the ripple output power during the steady state condition.

D. CASE 4: REAL TIME IRRADIANCE CONDITIONS

The performance of the proposed method under rapidly changing irradiance and constant temperature (25 oC) is studied using real-time data samples. The real-time data was gathered from the weather station, where it collects the irradiance data at a sample rate of 60 s using the sensor and it is stored in the database in 60 s intervals. Figure 9(a) shows the rapid changes in the irradiance on a particular day in early June month in 2022. In order to simulate abruptly changing irradiance, 40 data samples of irradiance are collected at regular intervals from 10:55 AM to 11:15 AM. The collected data is given as a step input and it is considered that the changes are occurring every 0.1 s as shown in Figure 9(b). The output power results of employing the conventional fixed small step size, large fixed step size, and the proposed method are shown in Figure 10. It can be seen clearly that, when there is a sudden change in irradiance, the proposed method offers a fast tracking time with lower ripple output power. Furthermore, the grid side results are tested with both the conventional and the proposed methods. It is assumed that the results are obtained as the system has been synchronised with the utility grid. Figure 11 and 12 show the d-q axis currents and the active and reactive power respectively. It can be seen clearly that the active power and active current follow the irradiance shape under rapid changes. This is due to the output reference voltage, Vdc,ref , from the MPPT being fed into the outer loop voltage control. Whereas the reactive power and reactive

current do not follow the irradiance shape due to the current controller qaxis, Iq,ref , being set equal to zero to ensure unity power factor operation. It is clear that by employing the proposed method, the grid side results and the PV side results are both improved in terms of their settling time and ripple output power.

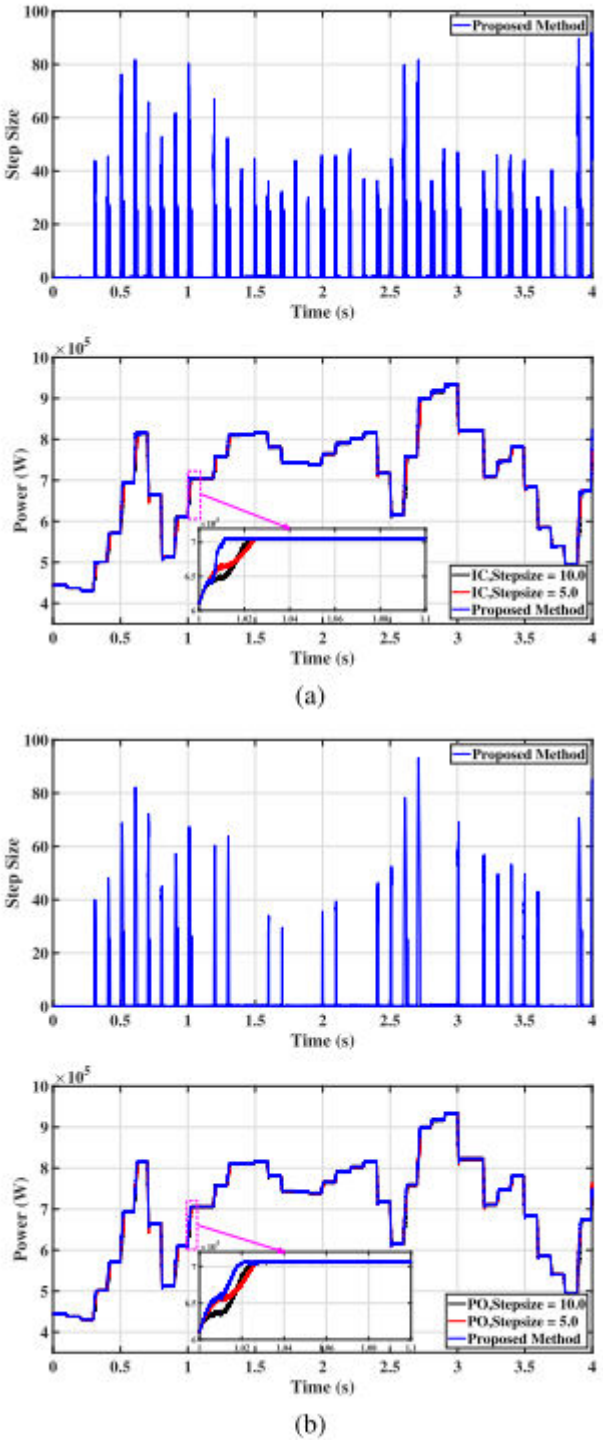

FIGURE 10. System response under real time irradiance conditions; (a) Proposed method step size and PV output power comparison for incremental conductance, and (b) Proposed method step size and PV output power comparison for perturb and observe.

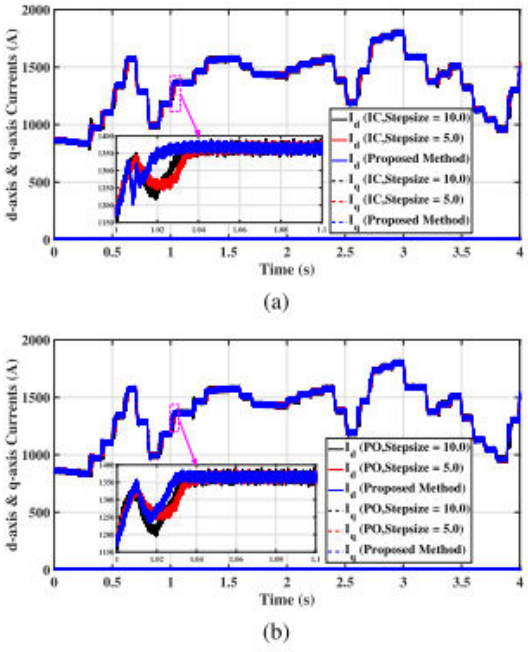

FIGURE 11. Grid side results: d-axis and q-axis currents comparison for (a) Incremental conductance, and (b) Perturb and observe.

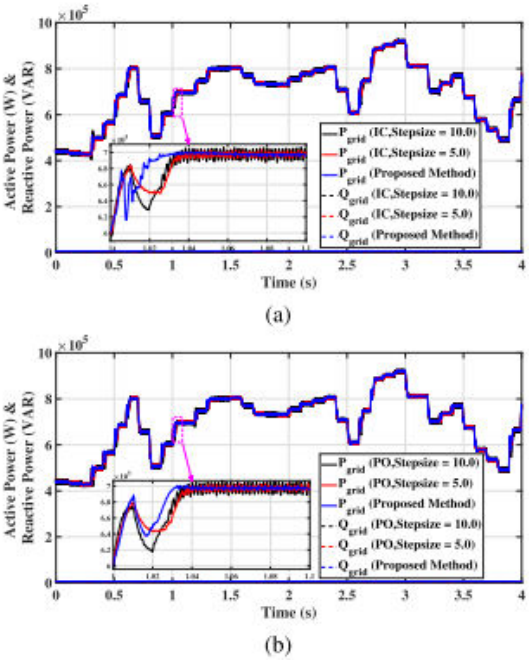

FIGURE 12. Grid side results: Active and reactive power comparison for (a) Incremental conductance, and (b) Perturb and observe.

VII. CONCLUSION

In this paper, the proposed method (PSO+IC and PSO+PO) are employed for a single-stage grid-connected PV system. The proposed method is developed based on penalizing the step size by optimizing a single objective function problem with constraints, such that to maximize the output power of the PV system. The accuracy of the proposed method is verified and confirmed by comparing it with the conventional methods (IC and PO). A detailed case study is carried out under standard test conditions, changing irradiance conditions, changing temperature conditions, and real-time irradiance conditions. It was found that the proposed method improves the system efficiency by reducing the settling time (i.e. faster tracking time) and reduces the ripple output power (i.e. less oscillation at steady state). In future work, a detailed experimental case study which includes the proposed MPPT and the actual power system network with a large scale singlestage grid connected PV system will be implemented to further validate the results.

REFERENCES

[1] F. Blaabjerg, R. Teodorescu, M. Liserre, and A. V. Timbus, ‘‘Overview of control and grid synchronization for distributed power generation systems,’’ IEEE Trans. Ind. Electron., vol. 53, no. 5, pp. 1398–1409, Oct. 2006, doi: 10.1109/TIE.2006.881997.

[2] Y. Huang, J. Wang, F. Z. Peng, and D.-W. Yoo, ‘‘Survey of the power conditioning system for PV power generation,’’ in Proc. 37th IEEE Power Electron. Spec. Conf., Jun. 2006, pp. 1–6.

[3] Y. Chaibi, A. Allouhi, M. Salhi, and A. El-Jouni, ‘‘Annual performance analysis of different maximum power point tracking techniques used in photovoltaic systems,’’ Protection Control Modern Power Syst., vol. 4, no. 1, pp. 1–10, Aug. 2019, doi: 10.1186/s41601-019-0129-1.

[4] W. Xiao and W. G. Dunford, ‘‘A modified adaptive Hill climbing MPPT method for photovoltaic power systems,’’ in Proc. IEEE 35th Annu. Power Electron. Spec. Conf., Jun. 2004, pp. 1957–1963.

[5] D. Sera, L. Mathe, T. Kerekes, S. V. Spataru, and R. Teodorescu, ‘‘On the perturb-and-observe and incremental conductance MPPT methods for PV systems,’’ IEEE J. Photovolt., vol. 3, no. 3, pp. 1070–1078, Jul. 2013.

[6] W. Ping, D. Hui, D. Changyu, and Q. Shengbiao, ‘‘An improved MPPT algorithm based on traditional incremental conductance method,’’ in Proc. 4th Int. Conf. Power Electron. Syst. Appl., Jun. 2011, pp. 1–4. [7] S. Dhar, R. Sridhar, and G. Mathew, ‘‘Implementation of PV cell based standalone solar power system employing incremental conductance MPPT algorithm,’’ in Proc. Int. Conf. Circuits, Power Comput. Technol. (ICCPCT), Mar. 2013, pp. 1957–1963.

[8] V. N. Lal, M. Siddhardha, and S. N. Singh, ‘‘Control of a large scale single-stage grid-connected PV system utilizing

MPPT and reactive power capability,'' in Proc. IEEE Power Energy Soc. Gen. Meeting, Jul. 2013, pp. 1–5.

[9] S. Ozdemir, N. Altin, and I. Sefa, ''Single stage three level grid interactive MPPT inverter for PV systems,'' Energy Convers. Manage., vol. 80, pp. 561–572, Apr. 2014.

[10] J. Ahmed and Z. Salam, ''An improved perturb and observe (P&O) maximum power point tracking (MPPT) algorithm for higher efficiency,'' Appl. Energy, vol. 150, pp. 97–108, Jul. 2015.

[11] X. Li, H. Wen, L. Jiang, W. Xiao, Y. Du, and C. Zhao, ''An improved MPPT method for PV system with fast-converging speed and zero oscillation,'' IEEE Trans. Ind. Appl., vol. 52, no. 6, pp. 5051–5064, Nov. 2016.

[12] X. Serrano-Guerrero, J. Gonzalez-Romero, X. Cardenas-Carangui, and G. Escriva-Escriva, ''Improved variable step size P&O MPPT algorithm for PV systems,'' in Proc. 51st Int. Universities Power Eng. Conf. (UPEC), Sep. 2016, pp. 1–6.

[13] A. I. M. Ali, M. A. Sayed, and E. E. M. Mohamed, ''Modified efficient perturb and observe maximum power point tracking technique for gridtied PV system,'' Int. J. Electr. Power Energy Syst., vol. 99, pp. 192–202, Jul. 2018.

[14] K. Saidi, M. Maamoun, and M. Bounekhla, ''A new high performance variable step size perturb-and-observe MPPT algorithm for photovoltaic system,'' Int. J. Power Electron. Drive Syst. (IJPEDS), vol. 10, no. 3, p. 1662, Sep. 2019.

[15] L. Shang, H. Guo, and W. Zhu, ''An improved MPPT control strategy based on incremental conductance algorithm,'' Protection Control Modern Power Syst., vol. 5, no. 1, pp. 1–8, Dec. 2020.

[16] M. Hebchi, A. Kouzou, and A. Choucha, ''Improved incremental conductance algorithm for MPPT in photovoltaic system,'' in Proc. 18th Int. Multi-Conf. Syst., Signals Devices (SSD), Mar. 2021, pp. 1271–1278.